Strategies for Detecting Biological Molecules on Titan. — **Source link** ↗

Catherine D. Neish, Ralph D. Lorenz, Elizabeth P. Turtle, Jason W. Barnes ...+5 more authors

Institutions: University of Western Ontario, Johns Hopkins University Applied Physics Laboratory, University of Idaho, Goddard Space Flight Center ...+2 more institutions

Topics: Titan (rocket family)

Related papers:

- Titan's global crater population: A new assessment

- Titan's surface at 2.18-cm wavelength imaged by the Cassini RADAR radiometer: Results and interpretations through the first ten years of observation

- Impact craters on Titan

- A model intercomparison of Titan's climate and low-latitude environment

- Astrobiology on Titan: Geophysics to Organic Chemistry

Share this paper: f 𝕏 in ✉

View more about this paper here: https://typeset.io/papers/strategies-for-detecting-biological-molecules-on-titan-37n24j58xw

2018

Strategies for detecting biological molecules on Titan

Catherine Neish
cneish@uwo.ca

Ralph Lorenz
The Johns Hopkins University Applied Physics Laboratory

Elizabeth Turtle
The Johns Hopkins University Applied Physics Laboratory

Jason Barnes
The University of Idaho

Melissa Trainer
Goddard Space Flight Center

See next page for additional authors

Citation of this paper:

Authors

Catherine Neish, Ralph Lorenz, Elizabeth Turtle, Jason Barnes, Melissa Trainer, Bryan Stiles, Randolph Kirk, Charles Hibbitts, and Michael Malaska

1

1 **Strategies for detecting biological molecules on Titan**

2

3 C.D. Neish[1], R.D. Lorenz[2], E. P. Turtle[2], J.W. Barnes[3], M. Trainer[4], B. Stiles[5], R.

4 Kirk[6], C. A. Hibbitts[2], M. J. Malaska[5]

5

6 [1]Department of Earth Sciences, The University of Western Ontario, London, ON,

7 N6A 5B7, Canada (Phone: 519-661-3188; E-mail: cneish@uwo.ca)

8 [2]The Johns Hopkins Applied Physics Laboratory, Laurel, MD 20723, USA

9 [3]Department of Physics, University of Idaho, Moscow, ID 83844, USA

10 [4]NASA Goddard Space Flight Center, Greenbelt, MD 20771, USA

11 [5]Jet Propulsion Laboratory, California Institute of Technology, Pasadena, CA,

12 91109, USA

13 [6]United States Geological Survey, Astrogeology Science Center, Flagstaff, AZ,

14 86001, USA

15 *Research Paper resubmitted to Astrobiology*

16

17 November 29, 2017

18

19 *Running title:* Detecting biomolecules on Titan

20

21   **Abstract**

22

23   Saturn's moon Titan has all the ingredients needed to produce "life as we know

24   it". When exposed to liquid water, organic molecules analogous to those found on

25   Titan produce a range of biomolecules such as amino acids. Titan thus provides a

26   natural laboratory for studying the products of prebiotic chemistry. In this work,

27   we examine the ideal locales to search for evidence of, or progression towards,

28   life on Titan. We determine that the best sites to identify biological molecules are

29   deposits of impact melt on the floors of large, fresh impact craters, specifically

30   Sinlap, Selk, and Menrva craters. We find that it is not possible to identify

31   biomolecules on Titan through remote sensing, but rather through in-situ

32   measurements capable of identifying a wide range of biological molecules. Given

33   the non-uniformity of impact melt exposures on the floor of a weathered impact

34   crater, the ideal lander would be capable of precision targeting. This would allow

35   it to identify the locations of fresh impact melt deposits, and/or sites where the

36   melt deposits have been exposed through erosion or mass wasting. Determining

37   the extent of prebiotic chemistry within these melt deposits would help us to

38   understand how life could originate on a world very different from Earth.

39

42

1. Introduction

43

44

45   Saturn's moon Titan has all the ingredients for life as we know it[1]. Titan's

46   dense nitrogen-methane atmosphere supports a rich organic photochemistry

47   (Hörst, 2017). Ultraviolet photons and charged particles dissociate the methane

48   and nitrogen in the atmosphere to produce a suite of carbon, hydrogen, and

49   nitrogen containing products ($C_xH_yN_z$), which eventually settle onto the surface.

50   These products have been observed in Titan's atmosphere by the *Voyager*

51   missions (Hanel et al., 1981; Kunde et al., 1981; Maguire et al., 1981) and in both

52   the atmosphere and on the surface by the *Cassini-Huygens* mission (Niemann et

53   al., 2005; Lavvas et al., 2008; Janssen et al., 2016).

54   Once on the surface, the products of Titan's photochemistry may react

55   with liquid water in certain circumstances. Titan's surface is on average too cold

56   for liquid water (~94 K – Fulchignoni et al., 2005), but transient liquid water

57   environments may be found in impact melts and cryolavas (Thompson and Sagan,

58   1992; O'Brien et al., 2005; Neish et al., 2006). When organic molecules found on

59   Titan's surface are exposed to liquid water, they quickly incorporate oxygen

60   (Neish et al., 2008; 2009) to produce a range of biomolecules that include amino

61   acids and possibly nucleobases (Neish et al., 2010; Poch et al., 2012; Cleaves et

62   al., 2014). Impact melts and cryolavas of different volumes - and hence, different

---

[1] Here and throughout this paper, we use the term "life as we know it" to refer to carbon-based life that uses water as a solvent.

63   freezing timescales (O'Brien et al., 2005; Davies et al., 2010) - give us a unique

64   window into the extent to which prebiotic chemistry can proceed over different

65   time scales.

66   Thus, Titan provides a natural laboratory for studying the products of

67   prebiotic chemistry. These products provide crucial insight into what may be the

68   first steps towards life in an environment that is rich in carbon and nitrogen, as

69   well as water. It is even possible that life arose on Titan and survived for a short

70   interval before its habitat froze. Alternatively, life may have developed in Titan's

71   subsurface ocean, and evidence of this life could be brought to the surface through

72   geophysical processes such as volcanism (Fortes, 2000). A new exploration

73   strategy is required to collect the results of these natural experiments; such

74   measurements are not possible with the currently available data from the *Voyager*

75   and *Cassini-Huygens* missions.

76   Even before *Cassini* reached the outer solar system, it was recognized

77   that a post-*Cassini* scientific priority, especially for astrobiology, would be to

78   access surface material for detailed investigation (Chyba et al., 1999; Lorenz,

79   2000). More recently, identifying "Planetary Habitats" was included as one of the

80   three crosscutting themes of the National Research Council's "Visions and

81   Voyages for Planetary Science in the Decade 2013-2022" (Space Studies Board,

82   2012). In addition, Titan is currently listed as one of six potential mission themes

83   for NASA's next New Frontiers mission[2]. Such a mission could be specifically

84   designed to identify the products of prebiotic chemistry on Titan's surface.

85   In this work, we determine the ideal locales to search for biomolecules

86   on Titan, and suggest mission scenarios to test the hypothesis that the first steps

87   towards life have already occurred there. In this scenario, we would consider a

88   substantial presence of biomolecules (i.e., compounds that are essential to life as

89   we know it) as either a compelling indicator of an advanced prebiotic

90   environment or as a possible sign of extinct (or more speculatively, extant) life.

91

92   **2. Geological settings for aqueous chemistry on Titan**

93

94   Liquid water is both a crucial source of oxygen and a useful solvent for the

95   generation of biomolecules on Titan's surface. Thus, if we wish to identify

96   molecular indicators of prebiotic chemistry on Titan, we need to determine where

97   liquid water is most likely to have persisted. Although Titan's average surface

98   temperature of ~94 K precludes the existence of bodies of liquid water over

99   geologic timescales (unless there is an active hotspot – see Schulze-Makuch and

100   Grinspoon, 2005), it does not rule out the presence of water on the surface for

101   short periods of time. We are likely to find transient liquid water environments on

102   the surface of Titan in two distinct geological settings: (1) cryovolcanic lavas and

---

[2] See https://newfrontiers.larc.nasa.gov.

103   (2) melt in impact craters. In addition, Titan's deep interior has a liquid water

104   layer perhaps hundreds of kilometers thick, which may also contain biomolecules

105   (Fortes, 2000; Iess et al., 2012). Samples of this ocean may be transported to the

106   surface through cryovolcanic processes before eventually freezing. Thus, if we

107   wish to find biomolecules on the surface of Titan, we should focus our search in

108   and around cryovolcanoes and impact craters.

109

110   *2.1 Cryovolcanoes*

111

112   On Titan, lavas are generally referred to as cryolavas, since they involve

113   the eruption of substances that are considered volatiles on the surface of Earth

114   (e.g., water, water-ammonia mixtures, etc.). Features suggested to be caused by

115   cryovolcanism were first discovered on the icy satellites during the *Voyager*

116   missions (e.g., Jankowski and Squyres, 1988; Showman et al., 2004). More recent

117   observations point to the existence of present-day activity on Enceladus (Porco et

118   al., 2006) and Europa (Roth et al., 2014; Sparks et al., 2017).

119   Two conditions must be met for cryovolcanic flows to be present on a

120   surface: liquids must be present in the interior and those liquids must then migrate

121   to the surface. Theoretical models of Titan's formation and evolution predict that

122   a substantial liquid water layer must still exist in its interior, provided a sufficient

123   amount of ammonia is present in the ocean (Tobie et al., 2005). Observations by

124   the *Cassini* mission have confirmed the presence of a liquid water subsurface

125   ocean. Measurements of the tidal love number by the Radio Science experiment

126   require that Titan's interior is deformable over its orbital period, consistent with a

127   global ocean at depth (Iess et al., 2012). In addition, the Permittivity, Wave and

128   Altimetry instrument on ESA's *Huygens* probe detected a electric current in

129   Titan's ionosphere, consistent with a Schumann resonance between two

130   conductive layers. The lower layer was estimated to lie 55-80 km below the

131   surface, suggestive of a salty, subsurface ocean (Béghin et al., 2012). Other

132   analyses of Titan's overall shape, topography, and gravity field are consistent

133   with an ice shell of this thickness overlying a relatively dense subsurface ocean

134   (Nimmo and Bills, 2010; Mitri et al., 2014)

135   The second requirement for cryovolcanism is for liquid to be transported

136   from the interior to the surface. One plausible way to transport lava is through

137   fluid-filled cracks. Mitri et al. (2008) proposed a model in which ammonia-water

138   pockets are formed through cracking at the base of the ice I shell. As these

139   ammonia-water pockets undergo partial freezing, the ammonia concentration in

140   the pockets would increase, decreasing the negative buoyancy of the ammonia–

141   water mixture. Unlike pure liquid water, a liquid ammonia-water mixture of

142   peritectic composition ($\rho = 946$ kg m^{-3}) is near-neutral buoyancy in ice ($\rho = 917$

143   kg m^{-3}) (Croft et al. 1988). Though these pockets could not easily become

144   buoyant on their own (given the difference in density of ~20-30 kg m^{-3}), they are

145   sufficiently close to the neutral buoyancy point that large-scale tectonic stress

146   patterns (tides, non-synchronous rotation, satellite volume changes, solid state

147   convection, or subsurface pressure gradients associated with topography) could

148   enable the ammonia-water to erupt effusively onto the surface. Evidence of such

149   stress patterns are observed on Titan (Cook-Hallet et al., 2015; Liu et al., 2016).

150   Any lava extruded in this way would likely have a peritectic composition near

151   that of pure ammonia dihydrate (33 wt. % ammonia).

152   We can test the hypothesis that cryolavas have erupted onto Titan's

153   surface by looking for morphological constructs on the surface consistent with

154   volcanism. The *Cassini* RADAR instrument has imaged approximately two-thirds

155   of the surface of Titan, producing views of the landscape with resolutions as good

156   as 350 m. Although it is difficult to conclusively identify cryovolcanic constructs

157   at these resolutions (Moore and Pappalardo, 2011), several features remain

158   difficult to explain through any other geologic process (Lopes et al., 2013). The

159   most intriguing of these features is Sotra Patera (part of a region formerly known

160   as Sotra Facula). This region includes the deepest pit and some of the highest

161   mountains on Titan, as well as the associated flow-like features of Mohini

162   Fluctus, a 200 km feature extending from Sotra Patera with a lobate edge (Figure

163   1). If Sotra Patera is indeed a volcanic construct, the lava flows there would be an

164   interesting location for studying the interaction of liquid water with organic

165   molecules on Titan's surface.

166   However, unless this region represents a persistent hot spot, it is unlikely

167   that the lava will remain liquid long enough for aqueous chemistry to produce

168   complex, biological molecules. (Thus far, no evidence of hot spots has been

169   observed on Titan – Lopes et al., 2013.) Flow lobes tens of meters thick in Mohini

170   Fluctus (Lopes et al., 2013) would likely cool over relatively short timescales: if

171   heat is lost only by conduction, the one-dimensional thermal conduction equation

172   predicts that it should take only one year for a ten-meter-thick flow of water or

173   ammonia dihydrate to completely freeze. Even a 200 m high cryovolcanic dome

174   that is 90 km in radius is expected to take only several hundred years to freeze

175   completely (Neish et al., 2006).

176   In addition, if these lavas have a peritectic composition close to that of

177   pure ammonia dihydrate, they would erupt close to a temperature of 176 K. This

178   would significantly affect reaction rates. In a 13 wt. % ammonia solution at 253

179   K, reactions between Titan haze analogues and ammonia-water have half-lives of

180   a few days (Neish et al., 2009). According to the Arrhenius equation, a reaction at

181   253 K with an activation energy of 50 kJ/mol would take 3×10^4 times longer in a

182   peritectic melt at 176 K. Thus, a reaction that took a few days to complete at the

183   higher temperature would take a few hundred years to complete at the lower

184   temperature. The aqueous chemistry in cryolavas may not have sufficient time or

185   energy to produce more complicated prebiotic molecules.

186   More speculatively, Titan's subsurface ocean may contain biomolecules,

187   or even simple life forms (Fortes, 2000). Evidence of such biology could be found

188   frozen in the cryovolcanic lavas on the surface of Titan. However, given the

189   uncertain presence of biomolecules in the subsurface ocean, and the challenges

190   inherent in transporting material to the surface, we judge the priority for

191   exploration should focus on another geologic setting where biomolecules are

192   more likely to be present: impact melt deposits.

193

194   *2.2 Impact craters*

195

196   When a comet or asteroid impacts a planet, energy becomes available to

197   melt its surface. Ponds and flows of melted crustal rock are observed in and

198   around impact craters on terrestrial planets (e.g. Hawke and Head, 1977). Models

199   suggest that melt should be produced on icy satellites as well (Pierazzo et al.,

200   1997; Artemieva and Lunine 2003; Kraus et al. 2011) and smooth regions at the

201   center of the largest craters on Ganymede have been interpreted to be solidified

202   impact melt (Jones et al., 2003; Bray et al., 2012).

203   Titan's atmosphere is capable of shielding the surface from smaller

204   impactors (Ivanov et al., 1997; Artemieva and Lunine, 2005; Korycansky and

205   Zahnle, 2005), so any projectile that does strike the surface must necessarily be

206   large. Such impactors would melt a substantial amount of Titan's crust. Artemieva

207   and Lunine (2003) conducted three-dimensional hydrodynamical simulations of

208   impacts into Titan's crust, and found that a 2 km icy projectile entering the

209   atmosphere at an oblique angle with a velocity of 7 km/s would generate 2-5 %

210   melt by volume within a transient crater 10-25 km in diameter. The amount of

211   melt increases with impact energy, so larger craters would contain a larger

212   percentage of melt by volume (Grieve and Cintala, 1992; Cintala and Grieve,

213   1998; Elder et al., 2012).

214   This melt could collect in the lowest parts of the crater, forming a sheet

215   several hundred meters thick. Given the higher density of liquid water compared

216   to the density of ice I, some melt could also drain into fractures in the crater floor

217   before freezing, forming the central pit features seen in craters on many icy

218   satellites (Elder et al., 2012). Using fracture volumes estimated from the gravity

219   anomalies observed over terrestrial impact craters, and assuming flow through

220   plane parallel fractures, Elder et al. (2012) estimated that melt will be retained for

221   Titan craters with diameters greater than ~90 km. However, this is a somewhat

222   idealized situation; in reality, fractures in the brecciated floor of an impact crater

223   are much more sinuous, with variable direction and width. If the fractures have a

224   tortuosity of two, only ~1/3 as much melt would drain (Elder et al., 2012).

225   (Tortuosity is the ratio of the length of the fracture to the depth of the fractured

226   region.) In addition, it is likely that fractures do not have a constant width, which

227   would cause the flow to slow through narrower passages, reducing the total

228   amount of melt volume drained. Since larger craters produce a larger fraction of

229   melt by volume than smaller craters (Grieve and Cintala, 1992), a reduced

230   drainage efficiency means that melt could also be retained for somewhat smaller

231   impact craters on Titan (larger craters would simply retain more melt than they

232   would if there was more efficient drainage).

233   The organics found on Titan's surface could then react with melt present

234   on the crater floor, in its ejecta blanket, or perhaps mixed with melt that drains

235   into fractures. Artemieva and Lunine (2003) found that a significant fraction

236   (10%) of Titan's organic surface layer would be only lightly shocked in an

237   impact. As a result, these organic molecules would be only partially altered,

238   providing reactants for any subsequent aqueous chemistry. In impact craters on

239   Earth, impact melt often incorporates large amounts of clastic material from non-

240   melted, but shocked target rocks (Osinski et al., 2017), suggesting there would be

241   efficient mixing between liquid water and organic clasts on Titan. In this way,

242   impact melts could provide "oases" for prebiotic chemistry to occur on Titan's

243   surface.

244   Once melted by the impact, any liquid water generated would begin to

245   cool to the ambient temperature of ~94 K. Thompson and Sagan (1992) were the

246   first to estimate the lifetime of melt pools generated in impacts on Titan. They

247   approximated the melt as a buried sphere of water freezing inward, and found

248   lifetimes of ~10^4 yr for a 10 km diameter crater, and ~10^6 yr for a 100 km

249   diameter crater. O'Brien et. al. (2005) refined the calculation using a thermal

250   conduction code, including more realistic geometries (such as sheets of melt

251   several hundreds of meters thick) and the possibility of water-ammonia melt

252   mixtures. With the melt fraction calculated by Artemieva and Lunine (2003), they

253   found somewhat shorter lifetimes of $\sim 10^2$-10^3 yr for a 15 km diameter crater, and

254   $\sim 10^3$-10^4 yr for a 150 km diameter crater. These lifetimes are considerably longer

255   than those for lava flows tens of meters thick, allowing more time for aqueous

256   chemistry to proceed. (Lifetimes could be reduced if a significant proportion of

257   the melt were to drain into the bottom of the crater, as discussed above.)

258   Impact melts would provide an excellent medium for aqueous chemistry

259   on Titan. In addition to having longer freezing timescales than cryovolcanic

260   flows, they are also likely to be emplaced at much higher temperatures. Melted

261   crustal rock (as opposed to water extruded from depth) is more likely to yield a

262   water-rich composition, with temperatures near the water liquidus (273 K), not

263   the ammonia-water peritectic (176 K). Temperatures may even exceed the

264   liquidus initially, given the large amounts of energy available from an impact. For

265   example, there is evidence for super-heating of several hundred Kelvins in impact

266   melts on Earth (Horz, 1965; El Goresy, 1965) and the Moon (Simonds et al.,

267   1976). This could increase the temperature of the melt above the liquidus,

268   accelerating the chemistry occurring in the melt ponds. Reactions between Titan

269   haze analogues and liquid water were roughly 20 times faster at 40°C than at 0°C

270   (Neish et al., 2008).

271   How many craters are available for such chemistry on Titan? We expect

272   impact cratering to be an important process in the Saturnian system, whose

273   satellites retain thousands of scars from past impacts (e.g., Kirchoff and Schenk,

274   2010). Before *Cassini* arrived at Saturn, the cratering history on Titan was

275   unknown from direct observations, so estimates of the cratering rate were made

276   by extrapolating the crater distributions observed on other Saturnian satellites, or

277   by predicting impact rates by comet populations. Such estimates suggested that at

278   least several hundred craters larger than 20 km in diameter should be present on

279   Titan (Zahnle et al. 2003). Now that *Cassini* RADAR has been able to observe

280   Titan's surface, an extreme paucity of craters is observed. Only 23 certain or

281   nearly certain craters and ~10 probable craters have been observed on Titan in this

282   size range, with a handful of smaller crater candidates (Wood et al., 2010; Neish

283   and Lorenz, 2012; Neish et al., 2016). This population has crater depths

284   consistently shallower than similarly sized fresh craters on Ganymede, suggestive

285   of extensive modification by erosion and burial (Neish et al., 2013). Although

286   aeolian infilling appears to be the dominant modification process on Titan, fluvial

287   erosion seems to play an important secondary role (Neish et al., 2016). In

288   addition, there is an almost complete absence of craters near Titan's poles, which

289   may be indicative of marine impacts into a former ocean in these regions (Neish

290   and Lorenz, 2014) or an increased rate of fluvial erosion (Neish et al., 2016).

291   We therefore judge that the best targets for observing the products of

292   aqueous – and possibly biological – chemistry on Titan are the floors of large,

293   relatively fresh impact craters. Fresh impact craters on Titan are subject to a

294   minimal amount of fluvial incision (which would expose the core of any impact

295   melt sheet), but little to no burial by sand or sediments (Neish et al., 2016). These

296   structures will contain the largest amount of impact melt, and that melt will be

297   easier to access with a spacecraft than the melt in more degraded craters (where it

298   is likely buried under a thick deposit of sediment).

299   To determine the best candidates for such studies, we consider the relative

300   degradation states of all 'certain' or 'nearly certain' craters on Titan with

301   diameters greater than 75 km (i.e., those craters most likely to retain impact melt).

302   As in Neish et al. (2013), we quantify the degradation state of a crater by

303   considering the relative depth of a Titan crater compared to a fresh, unmodified

304   crater on Ganymede with a similar diameter. The relative depth, R, is given by

305    $R(D) = 1 - d_t(D)/d_g(D)$ where $d_t(D)$ is the depth of a crater with diameter D on

306   Titan, and $d_g(D)$ is the depth of a crater with diameter D on Ganymede. A relative

307   depth of zero indicates the crater has the same depth as a crater on Ganymede and

308   is thus unmodified by erosion; a relative depth of one indicates the crater is

309   completely flat.

310   There is topography data for seven craters on Titan with D > 75 km. The

311   relative depths of five of these craters were previously reported in Neish et al.

312 (2013) and Neish et al. (2015). Topography data for the sixth crater – the ~80 km

313 diameter Selk crater – was obtained during *Cassini*'s T95 pass of Titan on 14

314 October 2013 (Figure 2a). A topographic profile was acquired through the center

315 of the crater using the SARTopo technique (Stiles et al., 2009). We calculated

316 depth, $d = h_1 – h_2$, by taking the difference between the highest point on the crater

317 rim and the lowest point on the crater floor, on both sides of the crater, d_1 and d_2

318 (Figure 2b). Systematic errors in height, dh_i, were propagated throughout the

319 analysis. These errors were determined from radar instrument noise and viewing

320 geometry (Stiles et al., 2009). Using this technique, the depth of Selk is 470 ± 90

321 m.

322   Topography data for the seventh crater – the ~140 km diameter Forseti –

323 was generated from stereo topography produced from overlapping radar images

324 from the T23 and T84 passes of Titan. Unfortunately, the stereo pair only covers

325 the northeast corner of the crater, so our depth estimate is based solely on the rim

326 heights and floor depths observed in this quadrant (Figure 3a). The floor elevation

327 is -2144 ± 35 m and the rim elevation is -1963 ± 54 m, for an average depth of

328 180 ± 60 m. In addition, there is a SARTopo profile through the northeast portion

329 of the crater, generated using data from *Cassini*'s T23 pass (Figure 3b).

330 Unfortunately, there is a data gap present on the crater floor, so we are only able

331 to calculate a minimum crater depth using this data set (Figure 3c). Using the

332 same technique as described for Selk, we found a *minimum* crater depth of $410 \pm$

333   50 m. This differs significantly from the depth derived from the stereo pair.

334   There are several possible reasons for this discrepancy. The crater floor

335   may appear to be level with the crater rim in the stereo pair due to a lack of

336   features on the floor. Identifiable features present in both images are necessary to

337   make stereo measurements. This situation could cause elevations on the crater

338   floor to be interpolated from the nearest rim points, artificially raising points on

339   the crater floor in the stereo data. In addition, impact craters often have large

340   variations in rim height (see, for example, Neish et al. 2017). By only measuring

341   one quadrant of the crater rim, we may not be getting a representative sample of

342   the rim height, thus biasing our result by using a lower than average portion of the

343   crater rim for depth measurements.

344   Updated topography data are also available for the ~100 km diameter

345   Hano crater. The data were generated from stereo topography produced from

346   overlapping radar images from *Cassini*'s T16 and T84 passes of Titan, and cover

347   more than half of the crater from the southwest quadrant to the northeast quadrant.

348   The result shows a crater with little noticeable topography (Figure 4a). In fact, the

349   average heights in the rim region (-1500 ± 170 m) and the average heights in the

350   floor region (-1510 ± 140 m) are nearly identical, suggesting that Hano crater is

351   essentially flat (R ~ 1). The initial depth estimate (d = 525 ± 100 m) by Neish et

352   al. (2013) using SARTopo only took into consideration one profile across the

353   southernmost rim of the crater, so it is possible that profile was not representative

354　of the crater as a whole. An updated SARTopo profile is now available, covering

355　both the northern and southern rim of Hano crater (Figure 4b). Using the same

356　technique as described for Selk, we found a new crater depth of 420 ± 40 m

357　(Figure 4c). As with Forseti, the stereo and SARTopo values differ considerably

358　for Hano crater, possibly for the same reasons outlined above. However, both of

359　the newly derived depths are lower than the initial estimate from Neish et al.

360　(2013). Thus, Hano appears to be more degraded than originally suggested, which

361　is consistent with its observed morphology in the RADAR data (Wood et al.,

362　2010).

363　　　　We summarize the relative depths of the seven craters in Table 1. Of

364　these, only two have relative depths < 0.6 for all current topography

365　measurements: Sinlap and Selk. We judge these to be the least degraded craters in

366　this size range. In terms of relative depth, Sinlap would be considered the

367　'freshest' crater on Titan, with R = 0.4 ± 0.2. It is difficult to assess the relative

368　depth of the largest crater on Titan, Menrva, since craters in this size range (D >

369　150 km) on icy satellites are associated with a sharp reduction in crater depth and

370　anomalous impact morphologies (Schenk, 2002). However, given the large

371　amount of impact melt expected in such a large crater, it remains a high priority

372　target for future exploration. The craters of interest are shown in Figure 5.

373

374　**3. Identifying biological molecules on Titan**

375

376   To identify biological molecules on Titan, it will be necessary to obtain

377   more detailed data than are currently available from past ground- and space-based

378   observations. As we describe below, the remote sensing data sets lack the spatial

379   and spectral resolution to make definitive conclusions about the composition of

380   Titan's surface. Compositional information regarding the potential presence of

381   biological molecules could be obtained from in-situ observations, but only if (a)

382   the associated instrumentation is designed for such a task, and (b) the surface

383   material can be obtained from the targeted regions described in Section 2. In this

384   section, we describe the difficulties in assessing surface composition remotely,

385   and describe possible approaches for in-situ detection of biological molecules.

386

387   *3.1 Detection by remote sensing?*

388

389   To date, Titan has been a focus of a number of spacecraft missions, as well

390   as numerous Earth-based telescopic observations. The collected data have

391   provided global observations of Titan's atmosphere and surface at a range of

392   spatial and spectral resolutions. However, it has remained a difficult challenge to

393   determine the composition of Titan's surface from remote observations (Hörst,

394   2017), for reasons we expand upon below.

395   *Pioneer 11* was the first spacecraft to encounter Saturn, and acquired the

396   first near range images of Titan in 1979 (Tomasko, 1980). This set the stage for

397   the *Voyager* missions, which flew by Saturn and Titan in 1980 (*Voyager* 1) and

398   1981 (*Voyager* 2), respectively (Stone, 1977). The *Voyager* missions returned

399   important information about Titan's atmospheric chemistry (e.g., Hanel et al.,

400   1981; Kunde et al., 1981; Maguire et al., 1981; Yung et al., 1984), but the

401   cameras on *Voyager* were unable to resolve any of the fine details of the surface

402   (Richardson et al. 2004). Such images were not obtained until the *Cassini-*

403   *Huygens* mission entered orbit around Saturn in 2004. Over the past thirteen years,

404   the *Cassini* RADAR, VIMS (Visual and Infrared Mapping Spectrometer), and ISS

405   (Imaging Science Subsystem) instruments have provided our first detailed looks

406   at the surface of Titan (Elachi et al., 2005; Barnes et al., 2005; Porco et al., 2005),

407   with the RADAR instrument providing the highest resolution views. However,

408   only ~2/3 of Titan's surface was imaged by the RADAR instrument by the end of

409   the Cassini mission, at resolutions of 350 - 2000 m. This limited spatial resolution

410   impacts our ability to differentiate surface units on Titan, and hence, determine

411   their differing compositions.

412   In addition to the limited spatial resolution available for Titan, there is

413   limited spectral resolution available for compositional analysis. Due to the

414   presence of Titan's thick nitrogen-methane atmosphere, remote spectroscopic

415   measurements are restricted to a discrete number of atmospheric 'windows',

416 where scattering and/or absorption are reduced (Lorenz and Mitton, 2002). For

417 example, the VIMS instrument on *Cassini* has only been able to image the surface

418 of Titan at seven atmospheric windows at wavelengths ranging between 0.94 and

419 5 μm (Brown et al., 2004).

420   High spectral resolution is crucial for the remote identification of surface

421 materials. The observation of key spectral features has provided essential

422 information about the composition of many planetary bodies, including the

423 identification of water ice on the Galilean satellites (Pilcher et al., 1972),

424 carbonates on Mars (Ehlmann et al., 2008), and hydroxyl on the Moon (Pieters et

425 al., 2009; Clark, 2009; Sunshine et al., 2009). With only a handful of wavelengths

426 available for surface analysis, similar identifications may be impossible on Titan.

427 The observations are further complicated by residual absorption and scattering

428 within Titan's atmospheric windows. For example, Hayne et al. (2014) found

429 strong atmospheric attenuation in the 2.7 μm window compared to the 2.8 μm

430 window, resulting in a reversal of the spectral slope expected for water ice.

431   These limitations are present for both orbital and aerial platforms (such as

432 a balloon or aircraft). This is true even though the amount of atmospheric

433 absorption between an aerial platform and the surface is much less than that

434 encountered by an orbiter. For example, the Huygens probe was able to image

435 Titan's surface at the meter scale from an altitude of 10 km (Tomasko et al.,

436 2005), but surface spectra could not be obtained outside of a few specific

437   spectroscopic windows (Tomasko et al., 2005). This is because at these altitudes,

438   there is little solar illumination for the surface to reflect, since much of the

439   sunlight has been absorbed or scattered by the overlying atmosphere (Tomasko et

440   al., 2005). McDonald et al. (2015) modeled the effect of methane absorption with

441   altitude, and found a slight widening of the spectral windows at altitudes closer to

442   the surface. However, they neglected to include the effects of atmospheric

443   scattering, and thus judge that the broadening they observe is at best an upper

444   limit. As a result, an airplane or balloon would provide little if any improvement

445   in the wavelengths available for spectroscopy over an orbiter. Given these

446   constraints, it would be difficult for a remote spectrometer to identify spectral

447   features associated with common biological molecules on Titan.

448   To test this hypothesis, we obtained reflectance spectra of several

449   molecules of biological interest in the laboratory. These include a pure powdered

450   sample of the amino acid glycine, a pure powdered sample of the amino acid

451   alanine, as well as a reflectance spectrum of a sample of glycine that had been

452   dissolved in water, frozen, and desiccated under vacuum (Figure 6a). We used an

453   ultra-high vacuum system that is able to obtain bidirectional reflectance spectra

454   (i=0°, e=30°) using a Bruker FTIR spectrometer. The spectrometer has a typical

455   resolution of 4 cm^{-1} (or ~10 nm at 5 μm, more than two times higher resolution

456   than VIMS), and a wavelength range limited to ~1.8 – 5.5 μm (see Hibbitts and

457   Szanyi, 2007).

458   When we compare the brightness of the laboratory spectra in the 2, 2.7,

459   2.8, and 5 μm atmospheric windows, we find they are almost indistinguishable

460   from each other. They are also rather featureless, unlike water ice, which shows a

461   prominent absorption band at 2.8 μm (Figure 6b). Moreover, given the purity of

462   these samples, the spectra presented here represent the absolute best-case scenario

463   for identifying biological molecules remotely. The concentration of biomolecules

464   in cryolavas and impact melts on Titan is likely to be much lower than the

465   concentrations measured in the laboratory. For example, hydrogen cyanide

466   (HCN), one biomolecule precursor (Ferris et al. 1978), is produced in Titan's

467   atmosphere at a rate of ~1.2 x 10^8 molecules cm-^{2} s^{-1} (Willacy et al. 2016). If

468   Titan's surface is ~1 Ga old (the upper limit estimated by Neish and Lorenz,

469   2012), we would expect ~10^{11} moles of HCN per km^2. For a 1 km^2 region of lava

470   or impact melt, this gives a HCN concentration of 1-10 M (for 10-100 m thick

471   layers of water). If the yield of glycine in such a solution is ~1% (Ferris et al.

472   1978), we would expect glycine concentrations of only 0.01-0.1 M in the lava or

473   impact melt. Further, the unique identification of particular molecules within a

474   complex mixture of organics is extremely challenging even with high sensitivity,

475   given multiple overlapping spectral features (see, for example, Clark et al., 2009).

476   Thus, remotely identifying biomolecules on Titan's surface from above or

477   within Titan's atmosphere would be difficult, even with an infrared camera that

478   has finer spatial and spectral resolution and wider spectral range than VIMS.

479

480   *3.2 Detection by in-situ sampling?*

481

482   Another approach for detecting biological molecules on Titan would be to

483   sample the surface in situ. This approach would require specific measurement

484   strategies. To date, only one spacecraft has acquired in situ information about

485   Titan's surface. In January 2005, the *Huygens* probe became the first (and only)

486   spacecraft to descend through Titan's atmosphere and land on its surface

487   (Lebreton et al., 2005). It provided detailed information about Titan's atmospheric

488   profile and chemistry (Fulchignoni et al., 2005; Niemann et al., 2005), as well as

489   information about Titan's surface properties (Niemann et al., 2005; Tomasko et

490   al., 2005; Zarnecki et al., 2005). The *Huygens* probe firmly identified methane

491   and ethane, and tentatively identified cyanogen (C_2N_2), benzene (C_6H_6), and

492   carbon dioxide (CO_2) on the surface of Titan (Niemann et al. 2010).

493   However, there has been as yet no identification of biological molecules

494   on the surface of Titan, and it is unlikely that such identifications will be possible

495   using the currently available data set. The *Huygens* probe was designed with

496   essentially no information about Titan's surface and was not guaranteed to survive

497   impact. As a result, it was not capable of precision landing near a site of

498   astrobiological interest, such as an impact crater or cryovolcano. Even if it had

499   landed in such an area, the mass resolution (1 amu) and mass range (1-140 amu)

500 of the *Huygens* GCMS (Gas Chromatograph Mass Spectrometer) were not suited

501 to the identification of biological molecules. Oxygenated organic molecules (e.g.,

502 $C_vH_xN_yO_z$) have mass differences much less than 1 amu compared to non-

503 oxygenated molecules of similar molecular weight (e.g., $C_{v+1}H_{x+4}N_y$).

504 Distinguishing between these products requires higher resolution mass

505 spectrometers (see Neish et al, 2008; 2009; Hörst et al., 2012; Hörst, 2017) and/or

506 a mechanism for separating different molecules with the same unit mass (Neish et

507 al., 2010; Cleaves et al., 2014). In addition, many amino acids and nucleobases

508 have masses in excess of 140 amu. Glutamine and glutamic acid fall into this

509 mass range, and they represent half of the amino acids identified in one

510 hydrolyzed sample of Titan haze analogues (Neish et al., 2010). Finally, and

511 perhaps most importantly, the surface material sampled by GCMS did not

512 encounter temperatures of more than ~150 K. As a result, no large complex

513 molecules were volatilized and ingested into the instrument (Lorenz et al. 2006).

514 The measurement of complex organics from a surface requires careful sample

515 handling and processing to enable analysis of these molecules without

516 degradation or conversion that obscures the chemical nature of the original

517 material. The *Huygens* probe was not designed to perform this type of

518 measurement.

519   Identification of biological molecules on Titan would require a spacecraft

520 capable of precision landing, equipped with a payload that is designed to identify

521   the composition and distribution of the organic molecules present within the

522   water-ice matrix. Existing or proposed spaceflight instrumentation could be used

523   to accomplish the in-situ detection of complex organics and potential

524   biomolecules in the Titan surface environment. Since the deployment of the

525   *Huygens* probe, two gas-chromatograph mass spectrometers have been flown that

526   exploit a solid sample acquisition and processing capability to pyrolyse samples

527   and measure a wide range of biological molecules (Goesmann et al., 2007;

528   Mahaffy et al., 2012). Both the *Rosetta* COSAC and *Mars Science Laboratory*

529   SAM instruments included chiral columns and derivatization agents to allow for

530   the volatilization of key functional groups in biologically interesting molecules,

531   such as amino acids, that would normally degrade or resist transport through the

532   gas chromatography columns (Freissinet et al., 2010). This analysis technique has

533   been demonstrated to successfully detect biomolecules in laboratory-based Titan

534   organic analogs that have undergone hydrolysis (Hörst et al., 2012; Poch et al.,

535   2012). The *ExoMars* MOMA instrument includes an additional capability of

536   laser-desorption mass spectrometry, which may have clear advantages in diverse

537   surface environments and for the measurement of large refractory organic

538   molecules (Siljestrom et al., 2014; Li et al., 2015; Goesmann et al., 2017).

539   Sampling and measurement in organic-laden ices, as proposed here, has

540   recently been discussed in the context of a science feasibility study of a landed

541   Europa mission (Hand et al., 2017). With the goal of searching for signs of life,

542 the lander's model payload includes an Organic Compositional Analyzer (OCA),

543 baselined to be a GCMS for the detection and identification of molecular

544 biosignatures, similar to those proposed as targets for Titan exploration. The

545 sampling and measurement approach discussed for Europa is highly applicable to

546 the Titan surface; in fact, the much-reduced radiation environment and anticipated

547 high density of organic molecules eases the requirements for chemical

548 characterization on Titan. Additional measurement approaches and sampling

549 implementations have been discussed with respect to the challenges that are

550 unique to cryogenic surfaces (Castillo et al., 2016).

551   In Section 2, we identified the highest priority targets for exploration by in

552 situ sampling systems: the floors of large, relatively unmodified impact craters

553 (specifically, Sinlap, Selk, and Menrva craters). Where, then, would be an ideal

554 place to sample within these craters? Much of Titan is covered in a thick layer of

555 organic molecules (Janssen et al., 2016), so not all impact melt deposits may be

556 accessible on a crater floor or in its ejecta blanket. We need to identify locations

557 where impact melt deposits have been recently exposed through erosion and/or

558 mass wasting.

559   To identify an appropriate sampling site, we consider a relevant terrestrial

560 analogue: Haughton crater in the Canadian Arctic. The 39 Ma Haughton impact

561 structure is a well preserved 23 km diameter crater in a polar desert, with little to

562 no obscuring vegetation (Osinski et al., 2005; Tornabene et al., 2005). Thus, it is

563   an excellent analogue for the study of craters on worlds that have experienced

564   moderate amounts of erosion, such as Mars or Titan. We note that the

565   geomorphology of the crater is what makes it a good analogue; the composition of

566   the substrate and chemical weathering experienced by the primarily carbonate

567   rocks at Haughton would be quite different from that experienced by a water-ice-

568   organic bedrock exposed to liquid hydrocarbons on Titan (Lorenz and Lunine,

569   1996). In addition, the periglacial processes that dominate the landscape in the

570   Canadian Arctic would not be found on Titan, where the temperatures are never

571   low enough for liquid hydrocarbons to freeze (Hanley et al., 2017).

572   Mapping in the interior of Haughton has revealed a large deposit of impact

573   melt breccia in the crater floor (the light-toned materials in Figure 7a). Using

574   geologic maps from Osinski et al. (2005), we estimate that this deposit represents

575   ~65% of the total area of the crater floor within 5 km of the crater centre (roughly

576   half the radius, R, of the crater), and ~20% of the crater floor within 10 km of the

577   crater centre (roughly one crater radius). Thus, a lander would have a high

578   probability of encountering impact melt if it were to land within ½ R of the crater

579   centre.

580   Notably, this melt deposit has been incised by multiple river channels

581   (Figure 7b), exposing fresh melt surfaces. Additional fluvial erosion and/or mass

582   wasting then brings samples of melt to the flat, smooth, alluvial plain at the

583   bottom of the crater (Figure 7c), where they would be easily accessible by a

584   lander. The benefit to accessing melt deposits at the bottom of river valleys is that

585   no drilling would be needed to reach an unaltered melt sample. Since liquid

586   hydrocarbons do not react chemically with water ice (Lorenz and Lunine, 1996),

587   even samples exposed to erosion and weathering in the Titan environment would

588   remain relatively pristine. We would also not expect any major alteration due to

589   high-energy electromagnetic radiation and/or charged particles, since ultraviolet

590   radiation and galactic cosmic rays do not penetrate all the way to the surface of

591   Titan (Hörst, 2017). Thus, any biological molecules present would be trapped

592   inside the chemically inert water ice, and so should be accessible when the sample

593   is ingested into a lander. Therefore, if we can identify river valleys on the floors

594   of Sinlap, Selk, and Menrva impact craters, these would be ideal landing sites.

595   The present resolution offered by the *Cassini* RADAR instrument is

596   insufficient to observe anything but the largest river channels; the *Huygens* probe

597   saw many more channels near its eventual landing site than are resolved in the

598   corresponding SAR images (e.g., Keller et al., 2008). Still, there is evidence for

599   fluvial erosion in many of Titan's craters; for example, there is evidence for large

600   river channels in the ejecta blankets of both Selk (Soderblom et al., 2010) and

601   Sinlap (Neish et al., 2015). Menrva is also characterized by many large fluvial

602   networks (Lorenz et al., 2008; Wood et al., 2010; Williams et al., 2011), which

603   likely expose impact melt deposits in the channel walls and as riverbed sediments.

604   Imaging from a mobile aerial platform, or perhaps from an orbiter designed to

605   perform such measurements, could help to identify where the deposits of interest

606   are most accessibly exposed.

607   In this work, we have remained agnostic as to the origin of the biological

608   molecules we seek to find in Titan's impact craters. However, future mission

609   planners may wish to differentiate between those biomolecules formed by abiotic

610   processes and those formed by biotic processes. There are several indicators that

611   may be able to differentiate between biomolecules of biotic origins from those of

612   abiotic origins. For example, one may use isotopic signatures to differentiate

613   between the two; life on Earth preferentially utilizes the lighter isotope of carbon,

614   ^{12}C, over the heavier isotope, ^{13}C (Cockell, 2015). One may also look for an

615   abundance of molecules with a single chirality; life on Earth uses only the L-

616   stereoisomer of amino acids, and not their mirror image, the D-stereoisomer

617   (McKay, 2016). Finally, one could consider the broader suite of molecules present

618   in the melt pond; abiotic processes typically produce smooth distributions of

619   organic material, while biologic processes select a highly specific set of molecules

620   (McKay, 2004).

621

622   **4. Conclusions**

623

624   Biomolecules similar to those found on Earth are likely present on Titan. To

625   identify and characterize them would require in-situ measurements of Titan's

626   surface material, obtained through precision targeting of a lander, equipped with

627   instrumentation capable of measuring a wide range of biological molecules. The

628   ideal landing sites would be the floors of Titan's largest, freshest impact craters,

629   where mass wasting and fluvial erosion expose fresh deposits of impact melt for

630   sampling. Impact craters are preferred over cryovolcanoes for a number of

631   reasons, chief among them the temperature of the aqueous medium; higher

632   temperatures at impact craters will increase reaction rates exponentially,

633   increasing the likelihood of forming complex biomolecules. Determining the

634   extent of prebiotic chemistry within these melt deposits would help us to

635   understand how life could originate on a world very different from Earth, and

636   shed light on prebiotic synthesis more generally.

637

638   **Acknowledgments**

639

647 structure. R. L. acknowledges the support of NASA PDART grant

648 NNX15AM23G.

649

650 **Author Disclosure Statement**

651

652 No competing financial interests exist.

653

654

655 **References**

656

657 Artemieva, N., and Lunine, J. (2003). Cratering on Titan: impact melt, ejecta, and

658 the fate of surface organics. *Icarus* 164:471–480.

659

660 Artemieva, N., and Lunine, J. I. (2005). Numerical calculations of the longevity

661 of impact oases on Titan. *Icarus* 173:243–253.

662

663 Barnes, J. W., Brown, R. H., Turtle, E. P., McEwen, A. S., et al. (2005). A 5-

664 micron-bright spot on Titan: Evidence for surface diversity. *Science* 310:92-95.

665

666 Barnes, J. W., Brown, R. H., Soderblom, L., Buratti, B. J., Sotin, C., Rodriguez,

667 S., Baines, K. H., Clark, R., and Nicholson, P. (2007). Global-scale surface

668 spectral variations on Titan seen from Cassini/VIMS. *Icarus* 186:242–258.

669

670 Barnes, J. W., Lemke, L., Foch, R., McKay, C. P., Beyer, R. A., Radebaugh, J., et

671 al. (2012). AVIATR—Aerial Vehicle for In-situ and Airborne Titan

672 Reconnaissance. A Titan airplane mission concept. *Experimental Astronomy*

673 33:55–127.

674

675 Béghin, C. B., Randriamboarison, O., Hamelin, M., Karkoschka, E., Sotin, C.,

676 Whitten, R. C., et al. (2012). Analytic theory of Titan's Schumann resonance:

677 Constraints on ionospheric conductivity and buried water ocean. *Icarus*

678 218:1028–1042.

679

680 Bray, V. J., Schenk, P. M., Melosh, H. J., Morgan, J. V., and Collins, G. S.

681 (2012). Ganymede crater dimensions: Implications for central peak and central pit

682 formation and development. *Icarus* 217:115–129.

683

684 Brown, R. H., Baines, K. H., Bellucci, G., Bibring, J. P., Buratti, B. J.,

685 Capaccioni, F., et al. (2004). The Cassini visual and infrared mapping

686 spectrometer (VIMS) investigation. *Space Science Reviews* 115:111–168.

687

688 Castillo, J. C., Y. Bar-Cohen, S. Vance, M. Choukroun, H. J. Lee, X. Bao, M.

689 Badescu, S. Sherrit, M. G. Trainer, and S. A. Getty (2016). Sample Handling and

690 Instruments for the In Situ Exploration of Ice-Rich Planets. In: *Low Temperature*

691 *Materials and Mechanisms*, edited by Y. Bar-Cohen, CRC Press, Boca Raton, FL,

692 pp. 229-270.

693

694 Chyba, C. et al. (1999). Europa and Titan: Preliminary Recommendations of the

695 Campaign Science Working Group on Prebiotic Chemistry in the Outer Solar

696 System. In: 30th *Lunar and Planetary Science Conference Abstracts*, Houston,

697   Texas, USA.

698

699   Cintala, M. J., and Grieve, R. A. F. (1998). Scaling impact-melt and crater

700   dimensions: Implications for the lunar cratering record. *Meteoritics & Planetary*

701   *Science* 33:889–912.

702

703   Clark, R. N. (2009). Detection of Adsorbed Water and Hydroxyl on the Moon.

704   *Science* 326:562 –564.

705

706   Clark, R.N., Curchin, J.M., Hoefen, T.M., and Swayze, G.A. (2009) Reflectance

707   spectroscopy of organic compounds: 1. Alkanes. *Journal of Geophysical*

708   *Research* 114:E03001.

709

710   Cleaves, H. J., Neish, C., Callahan, M. P., Parker, E., Fernández, F. M., and

711   Dworkin, J. P. (2014). Amino acids generated from hydrated Titan tholins:

712   Comparison with Miller-Urey electric discharge products. *Icarus* 237:182–189.

713

714   Cockell, C.S. (2015). *Astrobiology: Understanding life in the universe*. John

715   Wiley & Sons, Ltd., Sussex, UK, 449 pp.

716

717   Cook-Hallett, C., J. W. Barnes, S. A. Kattenhorn, T. Hurford, J. Radebaugh, B.

718   Stiles, and M. Beuthe (2015). Global contraction/expansion and polar lithospheric

719   thinning on Titan from patterns of tectonism. *Journal of Geophysical Research-*

720   *Planets* 120:1220–1236.

721

722   Coustenis, A., Atreya, S. K., Balint, T., Brown, R. H., Dougherty, M. K., Ferri, F.,

723   et al. (2008). TandEM: Titan and Enceladus mission. *Experimental Astronomy*

724   23:893–946.

725

726   Croft, S., Lunine, J., and Kargel, J. (1988). Equation of state of ammonia-water

727   liquid: Derivation and planetological applications. *Icarus* 73:279–293.

728

729   Davies, A.G., Sotin, C., Matson, D.L., Castillo-Rogez, J., Johnson, T.V.,

730   Choukroun, M., and Baines, K.H. (2010). Atmospheric control of the cooling rate

731   of impact melts and cryolavas on Titan's surface. *Icarus* 208:887-895.

732

733   Ehlmann, B. L., Mustard, J. F., Murchie, S. L., Poulet, F., Bishop, J. L., Brown,

734   A. J., et al. (2008). Orbital Identification of Carbonate-Bearing Rocks on Mars.

735   *Science* 322:1828–1832.

736

737   El Goresy, A. (1965). Baddeleyite and its significance in impact glasses. *Journal*

738   *of Geophysical Research* 70:3453–3456.

739

740   Elachi, C., et al. (2005). Cassini Radar Views the Surface of Titan. *Science*

741   308:970–974.

742

743   Elder, C. M., Bray, V. J., and Melosh, H. J. (2012). The theoretical plausibility of

744   central pit crater formation via melt drainage. *Icarus* 221:831–843.

745

746   Ferris, J., Joshi, P., Edelson, E., and Lawless, J. (1978). HCN: a plausible source

747   of purines, pyrimidines and amino acids on the primitive Earth. *Journal of*

748   *Molecular Evolution* 11:293–311.

749

750   Fortes, A. (2000). Exobiological Implications of a Possible Ammonia–Water

751   Ocean inside Titan. *Icarus* 146:444–452.

752

753   Freissinet, C., A. Buch, R. Sternberg, C. Szopa, C. Geffroy-Rodier, C. Jelinek,

754   and M. Stambouli (2010). Search for evidence of life in space: Analysis of

755   enantiomeric organic molecules by N,N-dimethylformamide dimethylacetal

756   derivative dependant Gas Chromatography-Mass Spectrometry. *Journal of*

757   *Chromatography A* 1217:731-740.

758

759   Fulchignoni, M., Ferri, F., Angrilli, F., Ball, A. J., Bar-Nun, A., Barucci, M. A., et

760   al. (2005). In situ measurements of the physical characteristics of Titan's

761   environment. *Nature* 438:785–791.

762

763   Goesmann, F., Rosenbauer, H., Roll, R., Szopa, C., Raulin, F., Sternberg, R., et al.

764   (2007). COSAC, The Cometary Sampling and Composition Experiment on

765   Philae. *Space Science Reviews* 128:257–280.

766

767   Goesmann, F., et al. (2017), The Mars Organic Molecule Analyzer (MOMA)

768   Instrument: Characterization of Organic Material in Martian Sediments,

769   *Astrobiology* 17:655-685.

770

771   Grieve, R.A.F., and Cintala, M.J. (1992). An analysis of differential impact melt-

772   crater scaling and implications for the terrestrial impact record. *Meteoritics &*

773   *Planetary Science* 27:526–538.

774

775   Hand, K.P., Murray, A.E., Garvin, J.B., Brinckerhoff, W.B., Christner, B.C,

776   Edgett, K.S, Ehlmann, B.L., German, C.R., Hayes, A.G., Hoehler, T.M.,

777   Horst, S.M., Lunine, J.I., Nealson, K.H., Paranicas, C., Schmidt, B.E., Smith,

778   D.E., Rhoden, A.R., Russell, M.J., Templeton, A.S., Willis, P.A., Yingst,

779   R.A., Phillips, C.B, Cable, M.L., Craft., K.L., Hofmann, A.E., Nordheim,

780   T.A., Pappalardo, R.P., and the Project Engineering Team (2017). *Report of*

781   *the Europa Lander Science Definition Team*. Posted February, 2017.

782

783   Hanel R, Conrath B, Flasar FM, Kunde V, Maguire W, Pearl J, Pirraglia J,

784   Samuelson R, Herath L, Allison M, Cruikshank D, Gautier D, Gierasch P, Horn

785   L, Koppany R, Ponnamperuma C (1981). Infrared observations of the saturnian

786   system from voyager 1. *Science* 212:192-200.

787

788   Hanley, J., Pearce, L., Thompson, G., Grundy, W., Roe, H., Lindberg, G.,

789   Dustrud, S., Trilling, D., and Tegler, S. (2017). Methane, Ethane, and Nitrogen

790   Stability on Titan. In: *48th Lunar and Planetary Science Conference Abstracts*,

791   The Woodlands, Texas, USA.

792

793   Hawke, B.R., and Head, J.W. (1977). Impact melt in lunar crater interiors. In:

794   *Impact and explosion cratering*, edited by D.J. Roddy, R.O. Pepin, and R.B.

795   Merrill, Pergamon Press, New York, NY, pp. 815.

796

797   Hayne, P. O., McCord, T. B., and Sotin, C. (2014). Titan's surface composition

798   and atmospheric transmission with solar occultation measurements by Cassini

799   VIMS. *Icarus* 243:158-172.

800

801   Hibbitts, C. A., and Szanyi, J. (2007). Physisorption of CO_2 on nonice materials

802   relevant to icy satellites. *Icarus* 191:371-380.

803

804   Hörst, S. M., Yelle, R. V., Buch, A., Carrasco, N., Cernogora, G., Dutuit, O.,

805   Quirico, E., Sciamma-O'Brien, E., Smith, M. A., Somogyi, A., Szopa, C.,

806   Thissen, R., and Vuitton, V. (2012). Formation of Amino Acids and Nucleotide

807   Bases in a Titan Atmosphere Simulation Experiment. *Astrobiology* 12:809–817.

808

809   Hörst, S. M. (2017). Titan's atmosphere and climate. *Journal of Geophysical*

810   *Research-Planets* 122:432–482.

811

812   Hörz F. (1965). Untersuchungen an Riesgläsern, *Beiträge zur Mineralogie und*

813   *Petrographie* 11:621–661.

814

815   Iess, L., Jacobson, R. A., Ducci, M., Stevenson, D. J., Lunine, J. I., Armstrong, J.

816   W., et al. (2012). The Tides of Titan. *Science* 337:457–459.

817

818   Ivanov, B. A., Basilevsky, A. T., and Neukum, G. (1997). Atmospheric entry of

819   large meteoroids: implication to Titan. *Planetary and Space Science* 45:993–

820   1007.

821

822   Jankowski, D., and Squyres, S. (1988). Solid-State Ice Volcanism on the Satellites

823   of Uranus. *Science* 241:1322–1325.

824

825   Janssen, M. A., Le Gall, A., Lopes, R. M., Lorenz, R. D., Malaska, M. J., Hayes,

826   A. G., et al. (2016). Titan's surface at 2.18-cm wavelength imaged by the Cassini

827   RADAR radiometer: Results and interpretations through the first ten years of

828   observation. *Icarus* 270:443–459.

829

830   Jones, K. B., Head, J. W., III, Pappalardo, R. T., and Moore, J. M. (2003).

831   Morphology and origin of palimpsests on Ganymede based on Galileo

832   observations. *Icarus* 164:197–212.

833

834   Keller, H. U., Grieger, B., Küppers, M., Schröder, S. E., Skorov, Y. V., and

835   Tomasko, M. G. (2008). The properties of Titan's surface at the Huygens landing

836   site from DISR observations. *Planetary and Space Science* 56:728–752.

837

838   Kirchoff, M.R. and Schenk, P. (2010). Impact cratering records of the mid-sized,

839   icy saturnian satellites. *Icarus* 206:485-497.

840

841   Korycansky, D. G., and Zahnle, K. J. (2005). Modeling crater populations on

842   Venus and Titan. *Planetary and Space Science* 53:695–710.

843

844   Kraus, R. G., Senft, L. E., and Stewart, S. T. (2011). Impacts onto H2O ice:

845   Scaling laws for melting, vaporization, excavation, and final crater size. *Icarus*

846   214:724–738.

847

848   Kunde, V. G., Aikin, A. C., Hanel, R. A., and Jennings, D. E. (1981). C4H2,

849   HC3N and C2N2 in Titan's atmosphere. *Nature* 292:686-688.

850

851   Lavvas, P. P., Coustenis, A., and Vardavas, I. M. (2008). Coupling

852   photochemistry with haze formation in Titan's atmosphere, Part II: Results and

853   validation with Cassini/Huygens data. *Planetary and Space Science* 56:67-99.

854

855   Lebreton, J.-P., Witasse, O., Sollazzo, C., Blancquaert, T., Couzin, P., Schipper,

856   A.-M., et al. (2005). An overview of the descent and landing of the Huygens

857   probe on Titan. *Nature* 438:758–764.

858

859   Li, X., R. M. Danell, W. B. Brinckerhoff, V. T. Pinnick, F. van Amerom, R. D.

860   Arevalo, S. A. Getty, P. R. Mahaffy, H. Steininger, and F. Goesmann (2015).

861   Detection of Trace Organics in Mars Analog Samples Containing Perchlorate by

862   Laser Desorption/Ionization Mass Spectrometry. *Astrobiology* 15:104-110.

863

864   Liu, Z.Y.C., Radebaugh, J., Christiansen, E.H., Harris, R.A., Neish, C.D., Kirk,

865   R.L. and Lorenz, R.D. (2016) The tectonics of Titan: Global structural mapping

866   from Cassini RADAR. *Icarus* 270:14-29.

867

868   Lopes, R. M. C., Kirk, R. L., Mitchell, K. L., Legall, A., Barnes, J. W., Hayes, A.,

869   et al. (2013). Cryovolcanism on Titan: New results from Cassini RADAR and

870   VIMS. *Journal of Geophysical Research-Planets* 118:416–435.

871

872   Lorenz, R.D. (2000) Post-Cassini Exploration of Titan: Science Rationale and

873   Mission Concepts. *Journal of the British Interplanetary Society* 53:218-234.

874

875   Lorenz, R., and Mitton, J. (2002). *Lifting Titan's Veil*. Cambridge University

876   Press, Cambridge, UK, 260 pp.

877

878   Lorenz, R. D., and Lunine, J. I. (1996). Erosion on Titan: Past and present. *Icarus*

879   122:79–91.

880

881   Lorenz, R. D., Niemann, H., Harpold, D., and Zarnecki, J. (2006). Titan's Damp

882   Ground: Constraints on Titan Surface Thermal Properties from the Temperature

883   Evolution of the Huygens GCMS inlet. *Meteoritics and Planetary Science*

884   41:1405-1414.

885

886   Lorenz, R. D., Lopes, R. M., Paganelli, F., Lunine, J. I., Kirk, R. L., Mitchell, K.

887   L., et al. (2008). Fluvial channels on Titan: Initial Cassini RADAR observations.

888   *Planetary and Space Science* 56:1132–1144.

889

890   Lorenz, R. D., Stofan, E., Lunine, J. I., Zarnecki, J. C., Harri, A. M., Karkoschka,

891   E., et al. (2012). MP3 - A meteorology and physical properties package to explore

892   air-sea interaction on Titan. In: 43rd *Lunar and Planetary Science Conference*

893   *Abstracts*, Houston, Texas, USA.

894

895   Maguire, W. C., Hanel, R. A., Jennings, D. E., and Kunde, V. G. (1981). C3H8

896   and C3H4 in Titan's atmosphere. *Nature* 292:683–686.

897

898   Mahaffy, P. R., Webster, C. R., Cabane, M., Conrad, P. G., Coll, P., Atreya, S. K.,

899   et al. (2012). The Sample Analysis at Mars Investigation and Instrument Suite.

900   *Space Science Reviews* 170:401–478.

901

902   McDonald, G.D., Corlies, P., Wray, J.J., Horst, S.M., Hofgartner, J.D., Liuzzo,

903   L.R., Buffo, J., and Hayes, A. G. (2015). Altitude-dependence of Titan's methane

904   transmission windows: Informing future missions. In: 46th *Lunar and Planetary*

905   *Science Conference Abstracts*, The Woodlands, Texas, USA.

906

907   McKay, C. P. (2004). What Is Life—and How Do We Search for It in Other

908   Worlds? *PLoS Biology*, 2:e302–4.

909

910   McKay, C. P. (2016). Titan as the Abode of Life. *Life* 6:8.

911

912   Mitri, G., Showman, A., Lunine, J., and Lopes, R. (2008). Resurfacing of Titan by

913   ammonia-water cryomagma. *Icarus* 196:216–224.

914

915   Mitri, G., Meriggiola, R., Hayes, A., Lefèvre, A., Tobie, G., Genova, A., et al.

916   (2014). Shape, topography, gravity anomalies and tidal deformation of Titan.

917   *Icarus* 236:169–177.

918

919   Moore, J. M., and Pappalardo, R. T. (2011). Titan: An exogenic world? *Icarus*

920   212:790–806.

921

922   Neish, C. D., and Lorenz, R. D. (2012). Titan's global crater population A new

923   assessment. *Planetary and Space Science* 60:26–33.

924

925   Neish, C. D., and Lorenz, R. D. (2014). Elevation distribution of Titan's craters

926 suggests extensive wetlands. *Icarus* 228:27-34.

927

928 Neish, C. D., Lorenz, R. D., O'Brien, D. P., and the Cassini RADAR Team.

929 (2006). The potential for prebiotic chemistry in the possible cryovolcanic dome

930 Ganesa Macula on Titan. *International Journal of Astrobiology* 5:57-65.

931

932 Neish, C. D., Somogyi, Á., Imanaka, H., Lunine, J. I., and Smith, M. A. (2008).

933 Rate Measurements of the Hydrolysis of Complex Organic Macromolecules in

934 Cold Aqueous Solutions: Implications for Prebiotic Chemistry on the Early Earth

935 and Titan. *Astrobiology* 8:273–287.

936

937 Neish, C. D., Somogyi, Á., Lunine, J. I., and Smith, M. A. (2009). Low

938 temperature hydrolysis of laboratory tholins in ammonia-water solutions:

939 Implications for prebiotic chemistry on Titan. *Icarus* 201:412–421.

940

941 Neish, C. D., Somogyi, Á., and Smith, M. A. (2010). Titan's Primordial Soup:

942 Formation of Amino Acids via Low-Temperature Hydrolysis of Tholins.

943 *Astrobiology* 10:337–347.

944

945 Neish, C. D., Kirk, R. L., Lorenz, R. D., Bray, V. J., Schenk, P., Stiles, B. W., et

946 al. (2013). Crater topography on Titan: Implications for landscape evolution.

947   *Icarus* 223:82–90.

948

949   Neish, C. D., Barnes, J. W., Sotin, C., MacKenzie, S., Soderblom, J. M., Le

950   Mouélic, S., et al. (2015). Spectral properties of Titan's impact craters imply

951   chemical weathering of its surface. *Geophysical Research Letters* 42:3746-3754.

952

953   Neish, C. D., Molaro, J. L., Lora, J. M., Howard, A. D., Kirk, R. L., Schenk, P., et

954   al. (2016). Fluvial erosion as a mechanism for crater modification on Titan. *Icarus*

955   270:114–129.

956

957   Neish, C. D., Herrick, R. R., Zanetti, M., and Smith, D. (2017). The role of pre-

958   impact topography in impact melt emplacement on terrestrial planets. *Icarus*

959   297:240–251.

960

961   Niemann, H. B., Atreya, S. K., Bauer, S. J., Carignan, G. R., Demick, J. E., Frost,

962   R. L., et al. (2005). The abundances of constituents of Titan's atmosphere from

963   the GCMS instrument on the Huygens probe. *Nature* 438:779–784.

964

965   Niemann, H. B., Atreya, S. K., Demick, J. E., Gautier, D., Haberman, J. A.,

966   Harpold, D. N., Kasprzak, W. T., Lunine, J. I., Owen, T. C., and Raulin, F.

967   (2010). Composition of Titan's lower atmosphere and simple surface volatiles as

968   measured by the Cassini-Huygens probe gas chromatograph mass spectrometer

969   experiment. *Journal of Geophysical Research* 115:E12006.

970

971   Nimmo, F., and Bills, B. G. (2010). Shell thickness variations and the long-

972   wavelength topography of Titan. *Icarus* 208:896–904.

973

974   O'Brien, D. P., Lorenz, R. D., and Lunine, J. I. (2005). Numerical calculations of

975   the longevity of impact oases on Titan. *Icarus* 173:243–253.

976

977   Osinski, G. R., Lee, P., Parnell, J., and Spray, J. G. (2005). A case study of

978   impact-induced hydrothermal activity: The Haughton impact structure, Devon

979   Island, Canadian High Arctic. *Meteoritics & And Planetary Science* 40:1859-

980   1877.

981

982   Osinski, G.R., Grieve, R.A.F., Bleacher, J.E., Pilles, E.A., and Tornabene, L.L.

983   (2017) Igneous rocks formed by hypervelocity impact. *Journal of Volcanological*

984   *and Geothermal Research* submitted.

985

986   Pierazzo, E., Vickery, A. M., and Melosh, H. J. (1997). A Reevaluation of Impact

987   Melt Production. *Icarus* 127:408–423.

988

989 Pieters, C. M., Goswami, J. N., Clark, R. N., Annadurai, M., Boardman, J.,

990 Buratti, B., et al. (2009). Character and Spatial Distribution of OH/H2O on the

991 Surface of the Moon Seen by M3 on Chandrayaan-1. *Science* 326:568–572.

992

993 Pilcher, C. B., Ridgway, S. T., and McCord, T. B. (1972). Galilean Satellites:

994 Identification of Water Frost. *Science* 178:1087–1089.

995

996 Poch, O., Coll, P., Buch, A., Ramírez, S. I., and Raulin, F. (2012). Production

997 yields of organics of astrobiological interest from H2O–NH3 hydrolysis of Titan's

998 tholins. *Planetary and Space Science* 61:114–123.

999

1000 Porco, C. C., Baker, E., Barbara, J., Beurle, K., Brahic, A., Burns, J. A., et al.

1001 (2005). Imaging of Titan from the Cassini spacecraft. *Nature* 434:159–168.

1002

1003 Porco, C. C., Helfenstein, P., Thomas, P. C., Ingersoll, A. P., Wisdom, J., West,

1004 R., et al. (2006). Cassini Observes the Active South Pole of Enceladus. *Science*

1005 311:1393–1401.

1006

1007 Richardson, J., Lorenz, R. D., and McEwen, A. (2004). Titan's surface and

1008 rotation: new results from Voyager 1 images. *Icarus* 170:113-124.

1009

1010   Roth, L., Retherford, K. D., Saur, J., Strobel, D. F., Feldman, P. D., McGrath, M.

1011   A., and Nimmo, F. (2014). Orbital apocenter is not a sufficient condition for

1012   HST/STIS detection of Europa's water vapor aurora. *Proceedings of the National*

1013   *Academy of Sciences* 111:E5123–E5132.

1014

1015   Schenk, P. M. (2002). Thickness constraints on the icy shells of the galilean

1016   satellites from a comparison of crater shapes. *Nature* 417:419–421.

1017

1018   Schulze-Makuch, D., and Grinspoon, D. (2005). Biologically enhanced energy

1019   and carbon cycling on Titan? *Astrobiology* 5:560–567.

1020

1021   Showman, A. P., Mosqueira, I., and Head, J. W., III. (2004). On the resurfacing of

1022   Ganymede by liquid–water volcanism. *Icarus* 172:625–640.

1023

1024   Siljestrom, S., C. Freissinet, F. Goesmann, H. Steininger, W. Goetz, A. Steele, H.

1025   Amundsen, and the AMASE11 Team (2014). Comparison of Prototype and

1026   Laboratory Experiments on MOMA GCMS: Results from the AMASE11

1027   Campaign. *Astrobiology* 14:780-797.

1028

1029   Simonds, C.H., Warner, J.L., and Phinney, W.C. (1976). Thermal regimes in

1030   cratered terrain with emphasis on the role of impact melt. *American Mineralogist*

1031   61:569–577.

1032

1033   Soderblom, J. M., Brown, R. H., Soderblom, L. A., Barnes, J. W., Jaumann, R.,

1034   Le Mouélic, S., et al. (2010). Geology of the Selk crater region on Titan from

1035   Cassini VIMS observations. *Icarus* 208:905–912.

1036

1037   Space Studies Board (2012). Vision and Voyages for Planetary Science in the

1038   Decade 2013–2022. National Academies Press. Available online at

1039   http://solarsystem.nasa.gov/docs/Vision_and_Voyages-FINAL.pdf.

1040

1041   Sparks, W.B., Schmidt, B.E., McGrath, M.A., Hand, K.P., Spencer, J.R., Cracraft,

1042   M., and Deustua, S.E. (2017). Active Cryovolcanism on Europa? *Astrophysical*

1043   *Journal Letters* 839:L18.

1044

1045   Stiles, B. W., Hensley, S., Gim, Y., Bates, D. M., Kirk, R. L., Hayes, A., et al.

1046   (2009). Determining Titan surface topography from Cassini SAR data. *Icarus*

1047   202:584–598.

1048

1049   Stofan, E., Lorenz, R. D., Lunine, J. I., Bierhaus, E. B., Clark, B., Mahaffy, P.R.,

1050   Ravine, M. (2013). TiME–The Titan Mare Explorer. In: *Proceedings of IEEE*

1051   *Aerospace Conference*, Big Sky, MT, March 2013, paper #2434.

1052

1053 Sunshine, J. M., Farnham, T. L., Feaga, L. M., Groussin, O., Merlin, F., Milliken,

1054 R. E., and A'Hearn, M. F. (2009). Temporal and Spatial Variability of Lunar

1055 Hydration As Observed by the Deep Impact Spacecraft. *Science* 326:565–568.

1056

1057 Thompson, W.R. and Sagan, C. (1992). Organic chemistry on Titan: surface

1058 interactions. In: *Proceedings of the Symposium on Titan*, 9–12 September 1991,

1059 Toulouse, France. ESA SP-338, pp. 167–176.

1060

1061 Tobie, G., Grasset, O., Lunine, J. I., Mocquet, A., and Sotin, C. (2005). Titan's

1062 internal structure inferred from a coupled thermal-orbital model. *Icarus* 175:496–

1063 502.

1064

1065 Tomasko, M. G. (1980). Preliminary results of polarimetry and photometry of

1066 Titan at large phase angles from Pioneer 11. *Journal of Geophysical Research:*

1067 *Space Physics* 85:5937–5942.

1068

1069 Tomasko, M. G., Archinal, B., Becker, T., Bézard, B., Bushroe, M., Combes, M.,

1070 et al. (2005). Rain, winds and haze during the Huygens probe's descent to Titan's

1071 surface. *Nature* 438:765–778.

1072

1073   Tornabene, L. L., Moersch, J. E., Osinski, G. R., Lee, P., and Wright, S. P.

1074   (2005). Spaceborne visible and thermal infrared lithologic mapping of impact-

1075   exposed subsurface lithologies at the Haughton impact structure, Devon Island,

1076   Canadian High Arctic: Applications to Mars. *Meteoritics & Planetary Science*

1077   40:1835–1858.

1078

1079   Trainer, M. G., Mahaffy, P. R., Stofan, E. R., Lunine, J. I., and Lorenz, R. D.

1080   (2012). Measuring the Composition of a Cryogenic Sea. *International Workshop*

1081   *on Instrumentation for Planetary Missions* 1683:1033.

1082

1083   Willacy, K., Allen, M. and Yung, Y. (2016). A new astrobiological model of the

1084   atmosphere of Titan. *The Astrophysical Journal* 829:79.

1085

1086   Williams, D.A., Radebaugh, J., Lopes, R.M.C., and Stofan, E. (2011)

1087   Geomorphologic mapping of the Menrva region of Titan using *Cassini* RADAR

1088   data. *Icarus* 212:744-750.

1089

1090   Wood, C. A., Lorenz, R., Kirk, R., Lopes, R., Mitchell, K., and Stofan, E. (2010).

1091   Impact craters on Titan. *Icarus* 206:334–344.

1092

1093   Yung, Y. L., Allen, M., and Pinto, J. P. (1984). Photochemistry of the atmosphere

1094   of Titan - Comparison between model and observations. *Astrophysical Journal*

1095   *Supplement Series* 55:465–506.

1096

1097   Zahnle, K., Schenk, P., Levison, H., and Dones, L. (2003). Cratering rates in the

1098   outer Solar System. *Icarus* 163:263–289.

1099

1100   Zarnecki, J. C., Leese, M. R., Hathi, B., Ball, A. J., Hagermann, A., Towner, M.

1101   C., et al. (2005). A soft solid surface on Titan as revealed by the Huygens Surface

1102   Science Package. *Nature* 438:792–795.

1103

1104 **Tables**

1105

1106 Table 1: Relative depths for seven 'certain' or 'nearly certain' craters on Titan
1107 with D > 75 km.

Crater	Diameter, D (km)	Depth, d (m)	Technique	Relative depth, R^a	Relative depth, R^c	Source of Depth Measurement
Soi	78 ± 2	240 ± 120	Stereo	0.78 ± 0.11	0.76 ± 0.12	Neish et al. (2015)
Selk	79 ± 7	470 ± 90	SARTopo	0.58 ± 0.08	0.53 ± 0.09	This paper
Sinlap	82 ± 2	640 (+160/-150)	SARTopo	0.43 (+0.14/-0.13)	0.36 (+0.16/-0.15)	Neish et al. (2013)
Hano	100 ± 5	420 ± 40	SARTopo	0.65 ± 0.03	0.56 ± 0.04	This paper
		~0	Stereo	~1	~1	This paper
Afekan	115 ± 5	455 (+175/-180)	SARTopo	0.62 (+0.15/-0.15)[b]	0.52 (+0.19/-0.19)	Neish et al. (2013)
Forseti	140 ± 10	180 ± 60	Stereo	0.85 ± 0.05[b]	0.80 ± 0.07	This paper
		>410 ± 50	SARTopo	< 0.66 ± 0.04[b]	< 0.55 ± 0.06	This paper
Menrva	425 ± 25	490 (+110/-120)	SARTopo	N/A	N/A	Neish et al. (2013)

1108 [a]Ganymede crater depths from Table 4 in Bray *et al.* (2012).

1109 [b]Assumed to have the same depth as a D = 100 km crater.

1110 [c]Ganymede crater depths from Figure 2b in Schenk (2002).

1111

1112

1113 **Figures**

1114
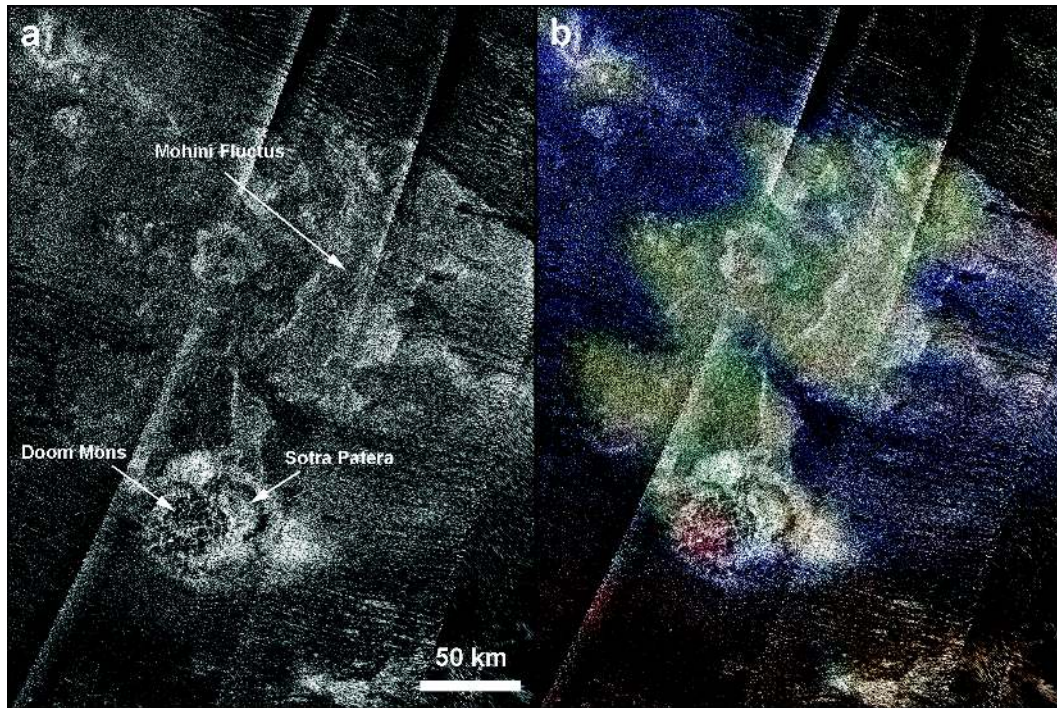
1115

FIG. 1. (a) *Cassini* RADAR image of Sotra Facula (centered near 13°S, 40°E). Sotra Patera (a 1700 m deep pit), Doom Mons (a 1450 m high mountain), and Mohini Fluctus (flow-like features tens of meters high) are labeled. **(b)** *Cassini* VIMS image of Sotra Facula, overlaid on the *Cassini* RADAR image (R: average over 4.90 to 5.07 μm, G: 2.02 μm, B: 1.28 μm). The dune fields are 'brown' in colour and 'blue' regions may be enriched in water ice. The 'yellowish-green' regions have an unknown composition, but may be a combination of water ice and organic molecules (Neish et al., 2015).

1124
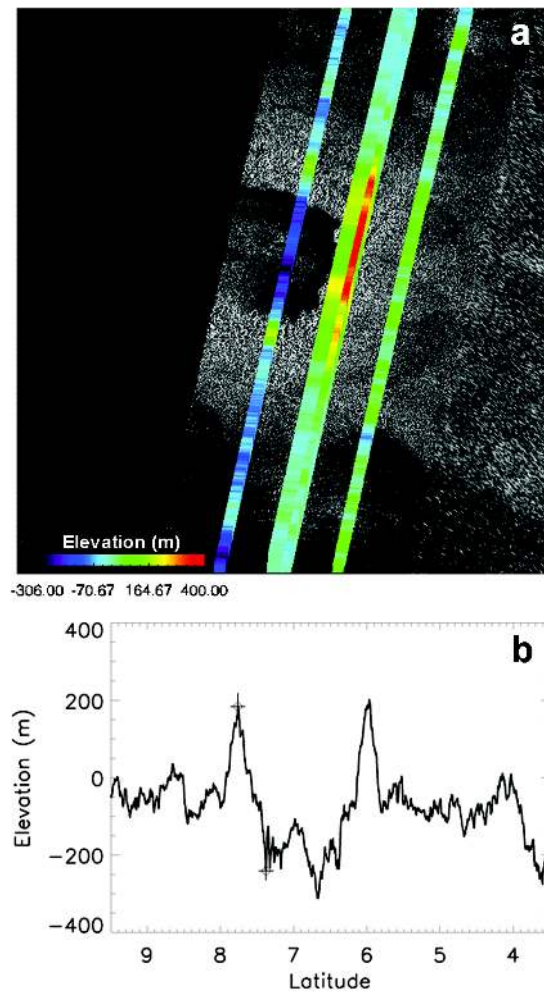
FIG. 2. **(a)** SARTopo profiles overlain on a *Cassini* RADAR image of Selk crater. The colours refer to the relative height at any point. North is up, and the image covers the range 3.5 – 9.5°N, 196 – 202°W. **(b)** The westernmost SARTopo profile from (a). Crosses indicate the points used to determine the depth of the northern half of the crater, d_1. Similar depth measurements were made in the southern half of the crater.
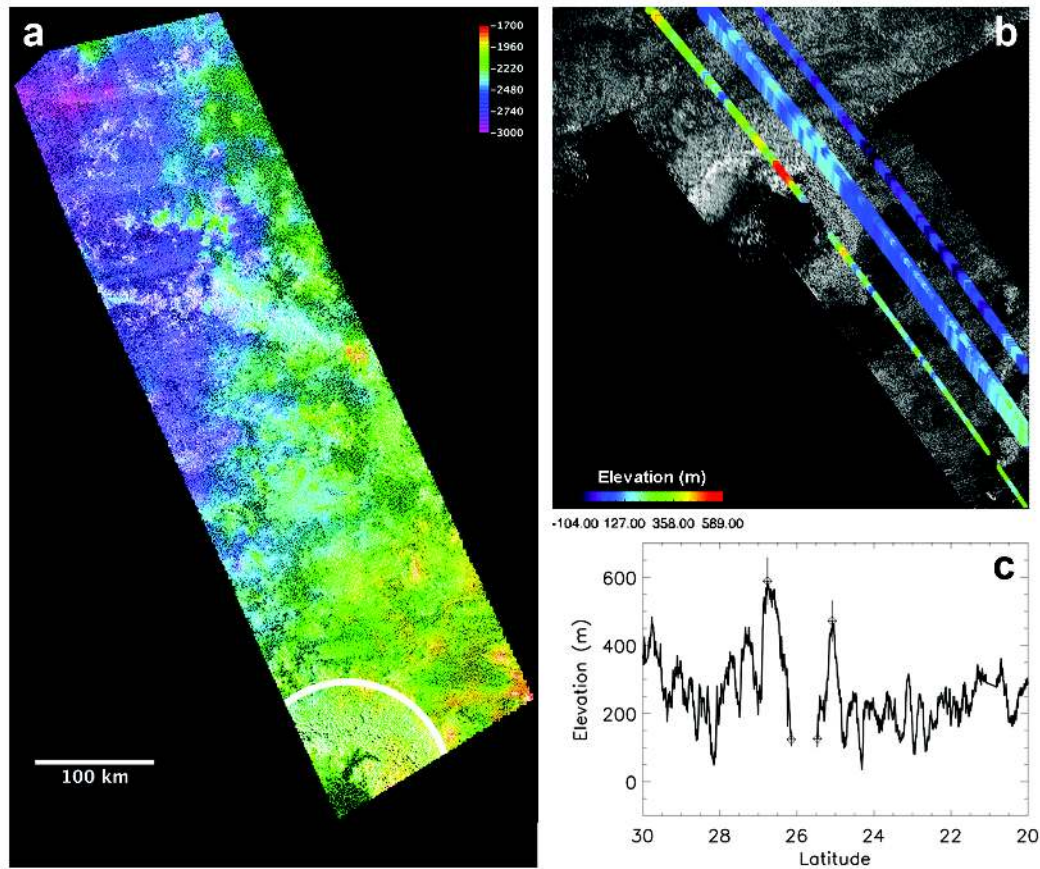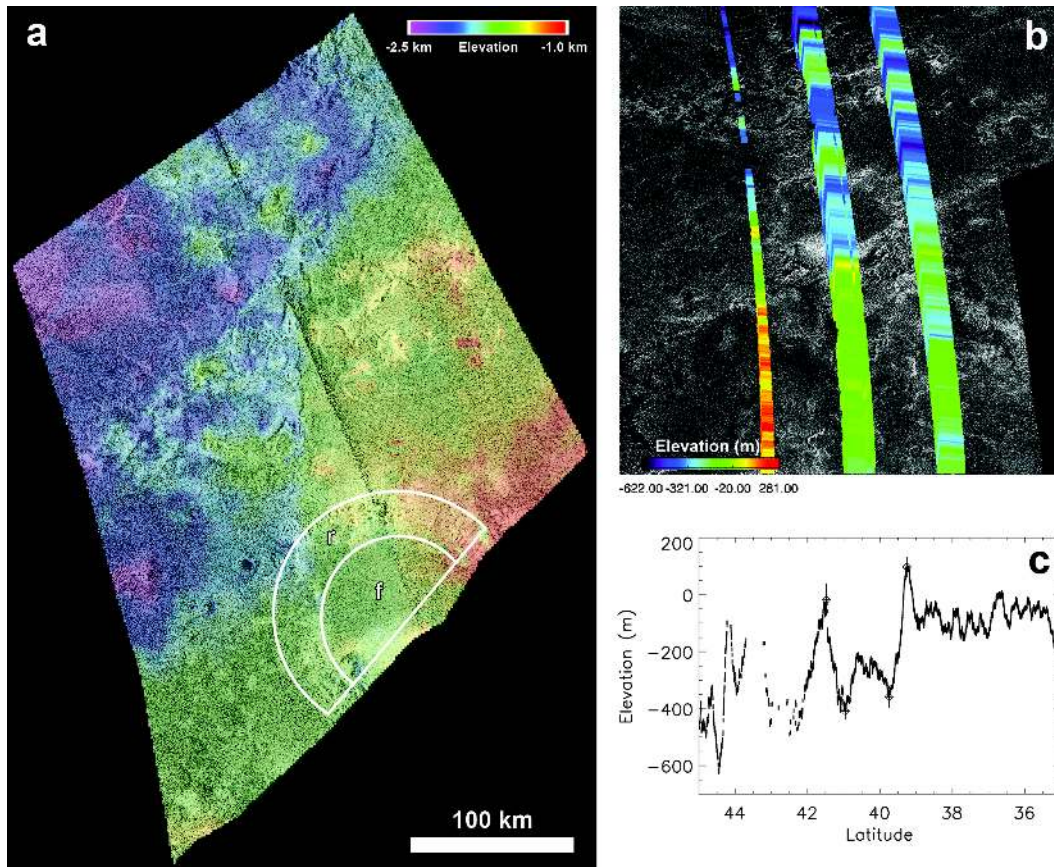
FIG. 3. (a) Stereo topography of Forseti crater in the overlapping region of the

T23 and T84 passes, overlain on a *Cassini* RADAR image. The crater is outlined

at bottom left. **(b)** SARTopo profiles overlaid on a *Cassini* RADAR image of

Forseti crater. The colours refer to the relative height at any point. North is up,

and the image covers the range 20 – 30°N, 5 – 15°W. **(c)** The westernmost

SARTopo profile from (a). Crosses indicate the points used to determine the

minimum depth of the crater.

FIG. 4. (a) Stereo topography of Hano crater in the overlapping region of the T16 and T84 passes, overlain on a *Cassini* RADAR image. The regions of Hano crater used to estimate the floor elevation (f) and rim elevation (r) are outlined at the bottom. **(b)** SARTopo profiles overlaid on a *Cassini* RADAR image of Hano crater. The colours refer to the relative height at any point. North is up, and the image covers the range 35 – 45°N, 340 – 350°W. **(c)** The center SARTopo profile from (a). Crosses indicate the points used to determine the depth of the crater.
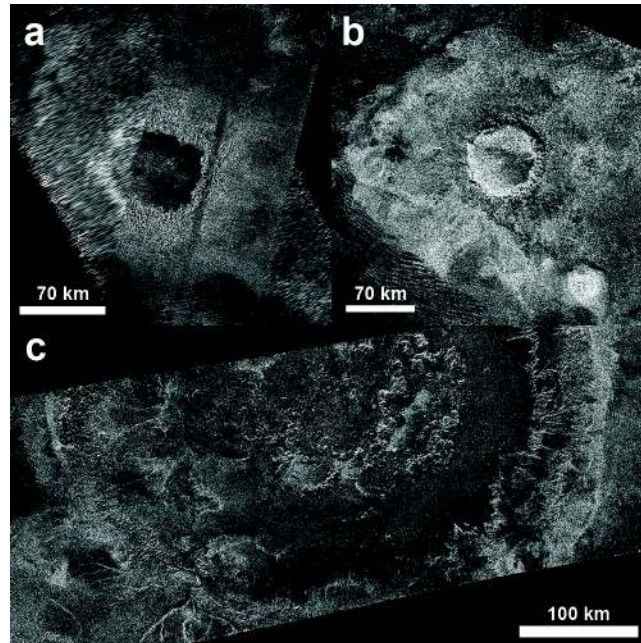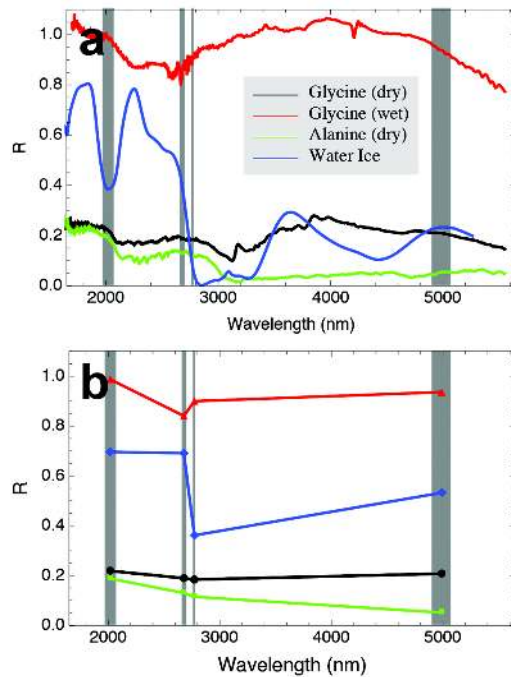
1151

1152 **FIG. 5.** These three large, relatively unmodified impact craters on Titan would be

1153 the best locations to identify biological molecules on its surface: **(a)** The 79 ± 7

1154 km diameter Selk (7°N, 198°W), **(b)** the 82 ± 2 km diameter Sinlap (11°N,

1155 16°W), (b) and **(c)** the 425 ± 25 km diameter Menrva (20°N, 87°W).

1156

1157

1158 **FIG. 6. (a)** Reflectance spectrum of powdered glycine (black), powdered alanine

1159 (green), pure water ice (blue), and glycine dissolved in water, frozen, and later

1160 warmed and desiccated under vacuum (red). Spectra of the amino acids have been

1161 obtained at both 100 K and room temperature, and they are identical for these

1162 materials. Shown in grey are the spectral windows through which VIMS can

1163 observe surface features on Titan. (Note that the 3.1-μm feature in the spectrum of

1164 dry glycine is due to water-ice build-up in the cryogenic infrared detector.) **(b)**

1165 Spectra of water ice (blue), "dry" glycine (black), "dry" alanine (green), and

1166 "wet" glycine (red) sampled in the four long-wavelength Titan atmospheric

1167 windows. The water-ice spectrum has been shifted vertically by 0.3 for ease of

1168 viewing.
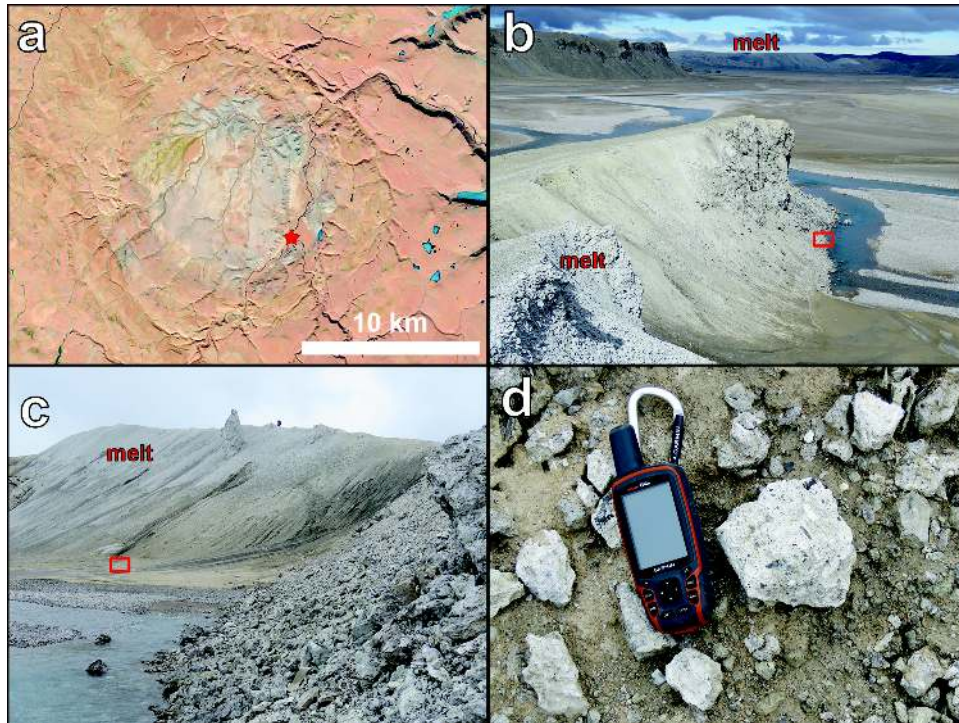
1169

FIG. 7. (a) Landsat-8 Operational Land Imager (OLI) natural colour image of

Haughton crater (75.4°N, 89.7°W) on Devon Island, Nunavut, Canada. The star

indicates the location of (b). North is up. **(b)** Lighter toned impact melt has been

exposed by the erosion of the impact crater interior by the Haughton River. View

is to the north. The box indicates the location where the author photographed

image (c). **(c)** Mass wasting and fluvial erosion brings samples of impact melt

breccia into the smooth river valley bottom. View is to the south, and a person is

visible on the ridgeline for scale. The box indicates the location where the author

photographed image (d). **(d)** If craters on Titan are similar in morphology to

Haughton, samples such as this ~10-cm cobble of impact melt breccia would be

safely accessible by a lander on the flat floor of a river valley.